

THE COXINEL SEEDED FREE ELECTRON LASER DRIVEN BY THE LASER PLASMA ACCELERATOR AT HZDR

M. E. Couprie[†], M. Labat, T. André, A. Berlioux, P. Berteaud, F. Blache, F. Bouvet, F. Briquez, C. de Oliveira, J. P. Duval, Y. Dietrich, M. El Ajouri, C. Herbeaux, N. Hubert, C. Kitégi, S. Lê, B. Leluan, A. Loulergue, F. Marteau, M. H. N'guyen, D. Oumbarek-Espino¹, D. Pereira, J. P. Ricaud, P. Rommeluère, M. Sebdaoui, K. Tavakoli, M. Valléau, M. Vandenbergh, J. Vétérán,

Synchrotron SOLEIL, Saint-Aubin, France,

A. Ghaith, A. Irman, S. Bock, Y. Y. Chang, A. Debus, C. Eisenmann, R. Gebhardt, S. Grams, U. Helbig, M. Kuntzsch, M. La Berge, R. Pausch, T. Püschel, S. Schöbel, K. Steiniger, P. Ufer, U. Schramm, Helmholtz-Zentrum Dresden – Rossendorf (HZDR), Dresden, Germany.

S. Corde, J. Gautier, J. P. Goddet, I. Andriyash, O. Kononenko, G. Lambert, V. Malka², P. Rousseau, A. Tafzi, C. Thaury, Laboratoire d'Optique appliquée (LOA), ENSTA Paris, CNRS, Ecole Polytechnique, Institut Polytechnique de Paris, Palaiseau, France

E. Roussel, Univ. Lille, CNRS, UMR 8523–PhLAM, Lille, France

¹ present address: Institute of Scientific and Industrial Research, Osaka University, Ibaraki, Japan

² Present address: Department of Physics of Complex Systems,
Weizmann Institute of Science, Rehovot, Israel

Abstract

Laser Plasma Accelerators know a tremendous development these recent years. Being able to reach up to ~ 100 GV/m, they open new perspectives for compact accelerators. Their performance can be qualified by a Free Electron Laser (FEL) application. We report here on the COXINEL (COherent X-ray source INferred from Electrons accelerated by lasers) seeded FEL in the UV using high-quality electron beam generated by the 150 TW DRACO laser. We present the COXINEL line developed at Synchrotron SOLEIL (France), the first results when installed at LOA and the seeded FEL achieved at HZDR.

INTRODUCTION

The FEL [1] following the laser invention [2, 3] was developed from infra-red [4], visible [5], UV-VUV [6, 7] in oscillator and coherent harmonic generation, to X-rays in the Self-Amplified Spontaneous Emission (SASE) after demonstrations at long wavelengths [8, 9], thanks to the high-quality electron beams provided by state-of-the-art photo-injectors and accelerators. Longitudinal coherence is improved with external seeding [10] and self-seeding [11]. In the Laser Plasma Acceleration (LPA) concept [12], following the laser discovery, an ultrashort and intense laser focused in a gas cell/jet excites a plasma oscillation, leads to a strong longitudinal accelerating field. High power lasers using chirped pulse amplification [13] boosted experimental demonstrations with hundred MeV range beams with few percent energy spread [14–16]. It opened the hope for driving FELs with LPA [17, 18] considering the use of a 5 fs- 1 PW laser leading to electron beams with 1.74 GeV, 0.1 % energy spread, 10 μrad divergence, 20 μm beam size, 1 nC charge and 150 kA peak current. LPA now reaches ~ 100 GV/m accelerating field with up to 8 GeV energies [19], 0.4%–1.2% energy spread [20], nC charge [21], [†] couprie@synchrotron-soleil.fr

[22], few fs bunch duration [23], and low emittance (\sim mm·mrad) [24]. These features, even though not simultaneously achieved, get closer to the FEL application requirements. Indeed, the first LPA based FEL has been demonstrated at SIOM with state-of-the-art LPA performance at 27 nm in the SASE regime [25]. The second LPA driven FEL has been achieved on COXINEL at HZDR in the seeded configuration at 267 nm [26], enabling for an improved longitudinal coherence.

COXINEL LINE

The COXINEL line was designed in 2010 considering a 200 MeV electron beam with a 1 mrad RMS divergence, 1 μm RMS beam size, 3.3 fs RMS bunch length, 34 pC charge, 1 % energy spread, 1 mm·mrad normalised emittance. The divergence is handled via a strong transverse focusing [27, 28] at the gas jet exit to prevent chromatic emittance growth [29]. The large energy spread is mitigated by a magnetic chicane, reducing the slice one by its decompression factor while elongating the bunch and reducing the peak current accordingly. Thanks to this energy/position correlation introduced in the chicane, the electron beam transverse focusing and the light progress along the undulator can be synchronized (chromatic matching) [28]. Modelling include electron beam transport with collective effects (space charge, coherent synchrotron radiation) [30], FEL sensitivity to parameters [31], FEL radiation. The chicane induced energy chirp coupled with undulator dispersion leads to a red-shifted FEL [33], and inference fringes between the seed and the FEL appear.

The COXINEL equipment have been prepared. The magnetic elements include the QUAPEVA permanent magnet quadrupoles for the initial strong focusing, with gradients up to 200 T/m and 50 % variability [33–35], four chicane electromagnetic dipoles for the slice energy spread reduction and the seed mirror insertion, an electromagnetic

dipole dump, four electromagnetic quadrupoles for the chromatic matching and four electromagnetic correctors. Short period high field 2 m long undulators [36] are used: first the spare SOLEIL In Vacuum Undulator of 20 mm period (IVU20), replaced by a Cryogenic permanent Magnet Undulator of 18 mm period (CPMU18#2) [37, 38], and by the IVU20#8 for the HZDR (maximum deflection parameter K_u of 2.47 at 4 mm gap). Diagnostics include five motorized electron beam imagers, two Turbo Integrating Current transformers (ICTs) [39], a spectrometer and an UV - CCD camera collecting the radiation at the line exit with a lens doublet for imaging the radiation along the undulator. The different parts, including the mechanical and vacuum ones, have been pre-assembled and aligned on the girders [40-42].

COXINEL FIRST RESULTS AT LOA

The COXINEL has been installed and aligned in 2016 in Salle Jaune at LOA, for using the 60 TW, 800 nm, 30 fs FWHM Ti:Sapphire laser for the LPA. The electrons were generated mainly in the ionization injection scheme with the laser focused into a supersonic jet filled a gas mixture (99% Helium, 1% Nitrogen), leading to broad energy spectra with typical 3.5 mrad slice vertical divergence. The electron beam has been rapidly transported. A Beam Pointing Alignment Compensation method, using the transfer matrix response of the line in BETA [43] and the translation of the QUAPEVA magnetic axis enables to independently adjust the electron beam position and the dispersion [44]. The residual skew quadrupolar components of the QUAPEVAs have been corrected [45, 46]. A slit was then inserted in the chicane to reduce the electron beam energy spread [47]. Further LPA improvements enabled to limit the divergence and improve the charge density.

Following first LPA based undulator radiation measurements [48-50], the COXINEL undulator radiation has been characterized, first with its transverse pattern [44] and then with its spectrum, enabling to adjust the resonant wavelength with the undulator gap [51] and to control the line spectral bandwidth by adjusting the energy spread via the slit width in the chicane, showing a good agreement with electron beam transport and SRW undulator radiation simulations [53] and analytical expressions.

The electrons and the seed (High order Harmonics generated in Gas at 200 and 270 nm, EKSMA kit at 270 nm), were spatially overlapped (imaging in the undulator), spectrally tuned (spectrometer) and synchronised (photodiode, spatial interference, Hamamatsu FESCA streak camera). Despite the electron beam improvements (1.5 mrad divergence and 1.5 pC/MeV) thanks to a laser upgrade, its quality was still too far from the baseline reference parameters for achieving the seeded FEL demonstration at LOA.

COXINEL RESULTS AT HZDR

Feasibilities studies in 2020-2021 covered the adaptation to the infrastructure, new electron beam measurements at 200 MeV, the energy of interest for a seeded FEL at 270 nm on COXINEL, the adjustment of the electron beam

transport and FEL modelling with GENESIS [54], an upgrade of the QUAPEVAs for better vacuum compatibility and the construction of the IVU#8 undulator.

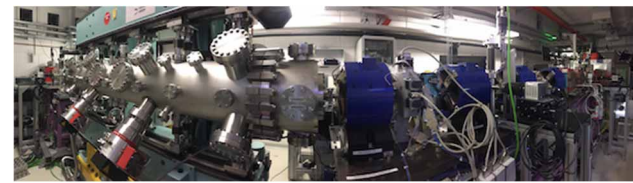


Figure 1: COXINEL line installed in HZDR LPA cave

The line was transported and installed in the HZDR cave in October 2021 (see Fig. 1), and aligned with a theodolite and a laser tracker, using the cross reference of the HZDR laser positions and fiducial SOLEIL ones.

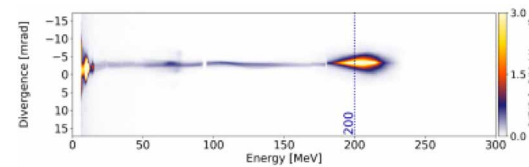


Figure 2: LPA e beam generated by the DRACO laser characterized on the magnetic spectrometer.

The HZDR LPA electron beam is operated with the 100 TW branch of the DRACO laser (30 fs FWHM, 2.1 J on target) in the tailored self-truncated ionization-induced injection [55] with 99 % He-1 % N₂ gas mixture, with a rather good charge and energy stability. Beam loading limits the energy spread to 6 % RMS at 188 MeV [21], a passive plasma lens by shaping the gas density profile keeps the divergence small (0.8 mrad in the horizontal plane), leading to 6.3 pC/MeV FWHM average charge density [26] (see Fig. 2), with a 14.8 fs FWHM estimated duration [23].

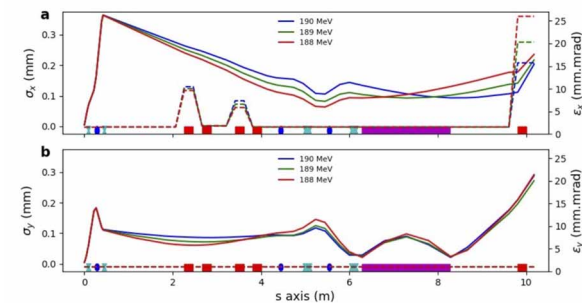


Figure 3: Electron beam envelops for different electron beam energies (ELEGANT simulations [56])

Electron beam was first transported in December 2021 (see envelops in Fig. 3) with up to 150 pC at the exit of the undulator. Undulator spontaneous emission was also measured, exhibiting the expected characteristics.

For the seed, a small fraction of the LPA driver laser is frequency tripled (EKSMA femtokit) with a group velocity compensation, spectrally and spatially filtered, stretched to 1 ps FWHM, resulting in a 3.9 nm (FWHM) bandwidth centered around 270 nm. It is injected with 0.8 μJ into the COXINEL line with an Al mirror, resulting in 0.5 μJ at the

undulator exit. The seed and undulator radiation are spectrally tuned looking at their spectra on the iHR320 Horiba-Jobin Yvon spectrometer, spatially overlapped by imaging in the undulator on a Hamamatsu ORCA-II UV camera and temporally synchronised with a FESCA 100 Hamamatsu streak camera from HZDR.

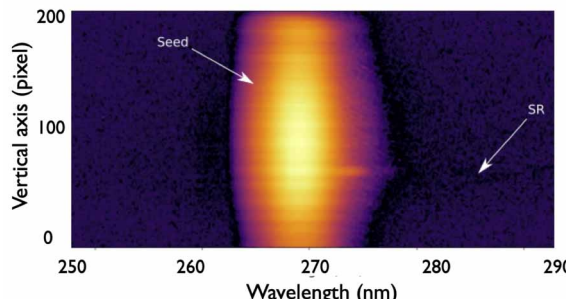


Figure 4: First seeded FEL signal.

During the first delay scan of FEL search in February 2022, the FEL signal was observed, as shown in Fig. 4 [26]. The FEL is red-shifted, as expected [32]. The FEL effect is confirmed by observing separately the seed, the spontaneous undulator radiation and the FEL, and by comparison with simulations. The quadratic charge dependence is confirmed. The FEL wavelength can be tuned with the undulator gap, but also with the delay because of the intrinsic red-shift and of the seed chirp. The expected fringes resulting from the phase-locked interference of the seed and the FEL are observed [26, 32], confirming the longitudinal coherence of the COXINEL seeded FEL. The FEL measurements have been reconfirmed during another experimental session in Nov. 2022.

CONCLUSION

We have demonstrated the first seeded LPA driven FEL on COXINEL installed at HZDR, evidencing longitudinal coherence [26]. Further electron beam improvements are foreseen for reaching shorter wavelengths.

ACKNOWLEDGEMENTS

Authors are supported by ERC (COXINEL (340015, M.-E. Couprise), X-Five (339128, V. Malka), M-PAC (715807, S. Corde), Fondation de la Coopération Scientifique (QUA-PEVA-2012-058T), Laserlab Europe V (contract no. 871124), Helmholtz Association (programme Matter and Technology, Accelerator Research and Development), Germany's Federal Ministry of Education and Research (BMBF) (Verbundforschung LADIAG), METEOR CNRS Momentum grant (E. Roussel), CPER P4S, Agence Nationale de la Recherche (ANR DYNACO, ANR-DFG ULTRASYNC), LABEX CEMPI ANR-11-LABX-0007).

REFERENCES

- [1] J. M. J. Madey, "Stimulated emission of Bremsstrahlung in a periodic magnetic field", *J. Appl. Phys.*, vol. 42, no. 5, pp. 1906-1913, 1971. doi:10.1063/1.1660466.
- [2] A. L. Schawlow and C. H. Townes, "Infrared and Optical Masers", *Phys. Rev. Lett.*, vol. 112, p. 1940. 1958. doi.org/10.1103/physrev.112.1940
- [3] T. H. Maiman, "Stimulated emission of radiation in ruby", *Nature*, vol. 187, p. 493. 1960. doi:10.1038/187493a0.
- [4] D. A. G. Deacon *et al.*, "First operation of a free-electron laser", *Phys. Rev. Lett.*, vol. 38, p. 892, 1977. doi:10.1103/physrevlett.38.892.
- [5] M. Billardon *et al.*, "Optical frequency multiplication by an optical klystron", *Phys. Rev. Lett.*, vol. 51, p. 1652, 2014. doi:10.1103/physrevlett.51.1652.
- [6] B. Girard *et al.*, "Optical frequency multiplication by an optical klystron", *Phys. Rev. Lett.*, vol. 53, p. 2405, 1984. doi:10.1103/physrevlett.53.2405.
- [7] R. Prazeres *et al.*, "Coherent harmonic generation in the vacuum ultraviolet spectral range on the storage ring ACO", *Nucl. Instrum. Methods*, vol. 272, p. 68, 1988. doi:10.1103/PhysRevLett.114.050511
- [8] A. L. Throop *et al.*, "Experimental results of a high gain microwave FEL operating at 140 GHz", *Nucl. Instrum. Methods*, vol. 272, p. 15, 1988. doi:10.1016/0168-9002(88)90187-8
- [9] P. Emma *et al.*, "First lasing and operation of an ångstrom-wavelength free-electron laser", *Nat. Photonics.*, vol. 4, p. 641, 2010. doi:10.1103/PhysRevLett.114.050511
- [10] L. H. Yu *et al.*, "High-gain harmonic-generation free-electron laser", *Science.*, vol. 289, no. 5, p. 5481, 2000. doi:10.1126/science.289.5481.932
- [11] A. A. Lutman *et al.*, "Demonstration of single-crystal self-seeded two-color X-ray free-electron lasers", *Phy. Rev. Lett.*, vol. 113, no. 5, p. 254801, 2013. doi:10.1103/physrevlett.110.134801.
- [12] T. Tajima and J. M. Dawson *et al.*, "Laser electron accelerator", *Phy. Rev. Lett.*, vol. 43, p. 267, 1979. doi.org/10.1103/PhysRevLett.43.267
- [13] D. Strickland and G. Mourou, "Compression of amplified chirped optical pulses", *Opt. Commun.*, vol. 55, p. 447, 1985. doi:10.1016/0030-4018(85)90151-8
- [14] S. P. Mangles *et al.*, "Monoenergetic beams of relativistic electrons from intense laser-plasma interactions", *Nature.*, vol. 431, p. 535, 2004. doi:10.1038/nature02939
- [15] C. G. R. Geddes *et al.*, "High-quality electron beams from a laser wakefield accelerator using plasma-channel guiding", *Nature.*, vol. 431, p. 538, 2004. doi:10.1038/nature02900
- [16] J. Faure *et al.*, "A laser-plasma accelerator producing monoenergetic electron beams", *Nature.*, vol. 431, p. 541, 2004. doi:10.1038/nature02963
- [17] F. Grüner *et al.*, "Design considerations for table-top, laser-based VUV and X-ray free electron lasers", *Appl. Phys. B*, vol. 86, p. 431, 2007. doi:10.1007/s00340-006-2565-7
- [18] K. Nakajima *et al.*, "Towards a table-top free-electron laser", *Nat. Phys.*, vol. 4, p. 92, 2008. doi:10.1038/nphys846
- [19] A. J. Gonsalves *et al.*, "Petawatt laser guiding and electron beam acceleration to 8 GeV in a laser-heated capillary discharge waveguide", *Phys. Rev. Lett.*, vol. 112, p. 084801, 2019. doi:10.1103/PhysRevLett.122.084801

- [20] W. T. Wang *et al.*, “High-brightness high-energy electron beams from a laser wakefield accelerator via energy chirp control”, *Phys. Rev. Lett.*, vol. 117, p. 124801, 2016.
doi:10.1103/PhysRevLett.117.124801
- [21] J. P. Couperus *et al.*, “Demonstration of a beam loaded nanocoulomb-class laser wakefield accelerator.”, *Nat. Commun.*, vol. 8, p. 487, 2017.
doi:10.1038/s41467-017-00592-7
- [22] J. Götzfried *et al.*, “Physics of high-charge electron beams in laser-plasma wakefields”, *Phys. Rev. Lett.*, vol. 114, no. 5, p. 050511, Feb. 1983.
doi:10.1103/PhysRevLett.114.050511
- [23] O. Zarini *et al.*, “Multi octave high-dynamic range optical spectrometer for single-pulse, longitudinal characterization of ultrashort electron bunches”, *Phys. Rev. Accel. Beams*, vol. 25, p. 012801, 2022.
doi:10.1103/PhysRevAccelBeams.25.012801
- [24] G. R. Plateau *et al.*, “Low-emittance electron bunches from a laser-plasma accelerator measured using single-shot X-ray spectroscopy”, *Phys. Rev. Lett.*, vol. 109, p. 064802, 2012.
doi:10.1103/PhysRevLett.109.064802
- [25] W. Wang *et al.*, “Free-electron lasing at 27 nanometres based on a laser wakefield accelerator”, *Nature*, vol. 595, p. 516, 2021. doi:10.1038/s41586-021-03678-x
- [26] M. Labat *et al.*, “Seeded free-electron laser driven by a compact laser plasma accelerator”, *Nature Photon.*, vol. 17, p. 150, 2022. doi:10.1038/s41566-022-01104-w
- [27] M. E. Coutrie *et al.*, “Towards a free electron laser based on laser plasma accelerators”, *Jour. Phys. B: At. Mol. Opt. Phys.*, vol. 47, no. 23, p. 234001, 2014.
doi:10.1088/0953-4075/47/23/234001
- [28] A. Loulergue *et al.*, “Beam manipulation for compact laser wakefield accelerator based free-electron lasers”, *New Jour. Phys.*, vol. 17, no. 2, p. 023028, 2015.
doi:10.1088/1367-2630/17/2/023028
- [29] K. Floettmann *et al.*, “Some basic features of the beam emittance”, *Phys. Rev. Accel. Beams*, vol. 6, p. 034202, 2003.
doi:10.1103/PhysRevSTAB.6.034202
- [30] M. Khojyan *et al.*, “Transport studies of LPA electron beam towards the FEL amplification at COXINEL”, *Nucl. Instr. Meth. A*, vol. 829, p. 260, 2016.
doi:10.1016/j.nima.2016.02.030i
- [31] M. Labat *et al.*, “Robustness of a plasma acceleration based Free Electron Laser”, *Phys. Rev. Accel. Beams*, vol. 21, p. 114802, 2018.
doi:10.1103/PhysRevAccelBeams.21.114802
- [32] M. Labat *et al.*, “Interferometry for full temporal reconstruction of laser-plasma accelerator-based seeded free electron lasers”, *New Journ. Phys.*, vol. 22, no. 1, p. 013051, 2020.
doi:10.1088/1367-2630/ab6878
- [33] C. Benabderrahmane, M. E. Coutrie, SOLEIL, F. Forest, O. Cosson Sigmaphi *et al.*, “Adjustable magnetic multipole”, *Patent Europe.*, EP 3189715 B1, published 2018-06-13, 2018, <https://bases-brevets.inpi.fr/fr/document/EP3189715/publications.html>
- [34] F. Marteau *et al.*, “Variable high gradient permanent magnet quadrupole (QUAPEVA)”, *Appl. Phys. Lett.*, vol. 111, p. 25, 2017. doi:10.1063/1.4986856
- [35] A. Ghaith *et al.*, “Tunable high gradient quadrupoles for a laser plasma acceleration based FEL”, *Nucl. Instrum. Meth. A*, vol. 909, p. 290, 2018.
doi:10.1016/j.nima.2018.02.098
- [36] A. Ghaith *et al.*, “Undulator design for Laser Plasma Based Free electron laser”, *Phys. Rept.*, vol. 937, p. 2184, 2021.
doi:10.1016/j.physrep.2021.09.001
- [37] C. Benabderrahmane *et al.*, “Development and operation of a PrFe₁₄B based cryogenic permanent magnet undulator for a high spatial resolution x-ray beam line”, *Phys. Rev. Accel. Beams.*, vol. 20, p. 033201, 2017.
doi:10.1103/PhysRevAccelBeams.20.033201
- [38] M. Valléau *et al.*, “Development of Cryogenic Permanent Magnet Undulators at SOLEIL”, *Synchrotron Radiat. News*, vol. 31, no. 3, p. 42, 2018.
doi:10.1080/08940886.2018.1460175
- [39] M. Labat *et al.*, “Electron and photon diagnostics for plasma acceleration-based FELs”, *J. Synchrotron Radiat.*, vol. 25, no. 1, p. 59, 2018. doi:10.1107/S1600577517011742
- [40] M. E. Coutrie *et al.*, “Towards free electron laser amplification to qualify laser plasma acceleration”, *Rev. Laser Eng.*, vol. 45, no. 2, p. 94, 2017.
- [41] M. E. Coutrie *et al.*, “An application of Laser Plasma Acceleration: Towards a Free Electron Laser amplification”, *Plasma Physics & Controlled Fusion*, vol. 58, no. 3, p. 034020, 2016.
doi:10.1088/0741-3335/58/3/034020
- [42] M. E. Coutrie *et al.*, “Towards a free electron laser using laser plasma acceleration on COXINEL”, in *Proc. SRI'18*, Taipei, Taiwan, Jun. 2018, *AIP Conf. Proc.*, vol. 2054, no. 1, p. 030034, 2019. doi:10.1063/1.5084597
- [43] J. Payet *et al.*, “BETA code”, *CEA-Saclay 2015*, <http://irfu.cea.fr/Sacm/logiciels/index6.php>
- [44] T. André *et al.*, “Control of laser plasma accelerated electrons for light sources”, *Nat. Comm.*, vol. 9, p. 1334, 2018.
doi:10.1038/s41467-018-03776-x
- [45] D. Oumbarek-Espinoz *et al.*, “Skew quadrupole effect of laser plasma electron beam transport”, *Appl. Sci.*, vol. 9, no. 12, p. 2447, 2019. doi:10.3390/app9122447
- [46] D. Oumbarek-Espinoz *et al.*, “COXINEL transport of laser plasma accelerated electrons”, *Plasma Physics & Controlled Fusion*, vol. 62, no. 3, p. 034001, 2020.
doi:10.1088/1361-6587/ab5fec
- [47] E. Roussel *et al.*, “Energy spread tuning of a laser-plasma accelerated electron beam in a magnetic chicane”, *Plasma Physics & Controlled Fusion*, vol. 62, no. 7, p. 074003, 2020. doi:10.1088/1361-6587/ab8ca0
- [48] H. P. Schlenvoigt *et al.*, “A compact synchrotron radiation source driven by a laser-plasma wakefield accelerator”, *Nat. Phys.*, vol. 4, p. 130, 2008. doi:10.1038/nphys811
- [49] M. Fuchs *et al.*, “Laser-driven soft-X-ray undulator source”, *Nat. Phys.*, vol. 5, p. 826, 2009.
doi:10.1038/nphys1404
- [50] M. P. Anania *et al.*, “An ultrashort pulse ultra-violet radiation undulator source driven by a laser plasma wakefield accelerator”, *Appl. Phys. Lett.*, vol. 104, p. 264102, 2014.
doi:10.1063/1.4886997
- [51] A. Ghaith *et al.*, “Tunable high spatio-spectral purity undulator radiation from a transported laser plasma accelerated electron beam”, *Sci. Rep.*, vol. 9, p. 19020, 2019.
doi:10.1038/s41598-019-55209-4

- [53] O. Chubar *et al.*, “A three-dimensional magnetostatics computer code for insertion devices”, *J. Synchrotron Rad.*, vol. 5, p. 481, 1998. doi:10.1107/S0909049597013502
- [54] S. Reiche *et al.*, “Genesis 1.3: a fully 3d time-dependent FEL simulation code”, *Nucl. Instrum. Meth. A.*, vol. 429, no. 1-3, p. 243, 1999. doi:10.1016/S0168-9002(99)00114-X
- [55] A. Irman *et al.*, “Improved performance of laser wakefield acceleration by tailored self-truncated injection”, *Plasma Physics & Controlled Fusion*, vol. 60, p. 044015, 2018. doi:0.1088/1361-6587/aaaef1
- [56] M. Borland, “Elegant: A flexible SDSS-compliant code for accelerator simulation”, Argonne National Laboratory, IL, USA, 2000.